J. Plasma Physics (2006), *vol.* 72, *part* 1, *pp.* 117–128.
doi:10.1017/S0022377805003843 first published online 25 Nov. 2005 Printed in the United Kingdom

Filamentation of Alfvén waves associated with transverse perturbation for compressible magnetohydrodynamics

M. MALIK and R. P. SHARMA†

Centre for Energy Studies, Indian Institute of Technology Delhi, New Delhi-110016, India
(rpsharma@ces.iitd.ernet.in)

(Received 2 February 2004, in revised form 24 January 2005 and accepted 27 January 2005)

Abstract. This paper presents an investigation of the filamentation process of a uniform plane Alfvén wave for a compressible magnetohydrodynamics case, when a transverse perturbation (perturbation having non-uniform intensity distribution in a plane perpendicular to the direction of wave propagation) is present on it. The physical mechanism of the filament formation is discussed in detail with the applications to the Solar wind turbulence and the coronal heating. The dependence of the critical field of the perturbation, its critical transverse size and the formation of filaments, on the plasma β, main Alfvén field and other parameters has been studied in detail.

1. Introduction

Alfvén waves are well-known solutions of ideal magnetohydrodynamics (MHD) equations, which assumes the concept of frozen-in field lines. These waves are believed to play a significant role in space plasmas, since they can propagate over large distances without dissipating (Spangler 1990; Spangler et al. 1988).

The surface temperature of the Sun is about 6000 K. While the temperature of the Solar corona is in excess 10^6 K. It has remained a mystery as to why the Solar corona is hotter than the Sun's surface. Closely related to the high temperature of the corona is the problem of the high speed of the Solar wind. Solar wind turbulence is a crucial element in coupling the lower coronal plasma and the Earth's magnetosphere, and in the transport of energetic particles throughout the Solar terrestrial environment. Hot high-speed Solar wind tends to contain highly Alfvénic fluctuations (i.e. the magnetic and velocity fluctuations are nearly equipartitioned in energy, and are heated as they move outwards in the heliosphere; see Tu and Marsch (1995) and Goldstein et al. (1995) for reviews). The filamentation process (hot spots formation) may provide a clue to the dissipation problem, because it is fast (catastrophic) way to transport energy at small scales. Therefore, the filamentation of Alfvén waves is important in the context of the Solar wind and the Solar corona.

† Author for correspondence.

The filamentation process has been studied in detail in the context of laser–plasma interaction (Kruer 1988). For a non-uniform laser beam, because of finite size of the beam, diffraction takes place. Nonlinearity present in the plasma also leads to a reduction of beam size. When these two effects balance each other, the laser beam will propagate without diverging or converging and is said to be in a self-trapped mode. The corresponding laser field (power) can be calculated and is termed as the critical field (power). If the laser field is more than the critical field, intense regions of the beam results, termed as filaments or hot spots. The filament formation is also expected to take place if the main laser beam is uniform and a non-uniform perturbation is present on the main laser beam.

Champeaux et al. (1997, 1998) have studied the filamentation of Alfvén waves in the framework of the Hall-MHD. Champeaux et al. (1998) studied the filament formation numerically when the transverse perturbation is periodic. Lavender et al. (2001) studied the filamentation of Alfvén waves numerically within the framework of a derivative nonlinear Schrödinger equation (DNLS), in three dimensions, when the initial circular Alfvén wave is perturbed by a broad-spectrum noise. Recently, Laveder et al. (2002) have also studied the filamentation of dispersive Alfvén waves by numerically solving the full Hall-MHD equations. They superimpose to the Alfvén pump density disturbances whose Fourier modes have random phases and random amplitudes bounded from above by a Gaussian profile. However, Alfvén waves in a resistive MHD plasma also show filamentation following the parametric instability (Del Zanna et al. 2001). Most of these works deal with the numerical simulations, and the details such as the coupling between the main Alfvén wave and the perturbation, different parameters governing this coupling, the dynamics of the perturbation and the parameters on which its filamentation depends need more research. In the present paper, we have investigated the filamentation of Alfvén waves in a compressible MHD plasma.

This paper presents an investigation of the filamentation process of a uniform plane Alfvén wave in a compressible MHD case when a transverse perturbation (perturbation having non-uniform intensity distribution in a plane perpendicular to the direction of propagation) is present on it. The physical mechanism of filament formation is discussed in detail with applications to the Solar wind turbulence and coronal heating. The dependence of the critical field of the perturbation, its critical transverse size and the formation of filaments on the plasma β, main Alfvén field and other parameters have been studied in detail.

In the present study, we have considered a plane Alfvén wave propagating along the z-direction. The main Alfvén wave and the perturbation are collinear and propagating in the same direction. The initial structure of the perturbation is taken to be Gaussian in a plane transverse to the direction of propagation. The main Alfvén wave and the perturbation are not necessarily in phase initially. Therefore, we have assumed a finite phase angle between the two (denoted by an angle φ). In Sec. 2, we present the model equations governing the dynamics of the main Alfvén wave and the perturbation. We have also obtained a solution of these model equations. The formation of filaments and the dependence of their intensity and their separation on various parameters for the Solar wind and Solar corona parameters is illustrated. A discussion of the results and their physical interpretation is presented in Sec. 3, where conclusions for the present investigation are also given.

2. Model equations and solutions

Consider a small amplitude Alfvén wave propagating along the magnetic field, assumed in the z-direction. Introducing the new set of variables, $X = \mu x$, $Y = \mu y$, $\xi = \mu^2 z$, using multi-scale expansion, and taking the linear polarization along y-axis (i.e. **B** $(0, B, 0)$ of the Alfvén wave), one can write the following equation in the steady state (Champeaux et al. 1999) in compressible MHD, without the Hall term,

$$i\partial_\xi B + \frac{1}{2k(1-\beta)}\frac{\partial^2 B}{\partial y^2} + \frac{(4\beta+1)}{4\beta}k|B|^2 B = 0. \tag{1}$$

Here the symbols have their usual meanings (Champeaux et al. 1998). Let a perturbation ($\mathbf{B}_1$), polarized along the y-axis, be superimposed on the main plane Alfvén wave ($\mathbf{B}_0$). The intensity distribution of the perturbation at $\xi = 0$, is assumed to be of the form

$$\mathbf{B}_1 \cdot \mathbf{B}_1^* = \mathbf{B}_{100}^2 \exp\left(-\frac{y^2}{r_0^2}\right). \tag{2}$$

It should be mentioned here that the perturbation $\mathbf{B}_1$ (modulating agent) can be any perturbation, for example due to fluctuation of the background field.

Here r_0 is the transverse scale size of the perturbation. Using (1), the perturbation field will satisfy the following equation:

$$i\partial_\xi B_1 + \frac{1}{2k(1-\beta)}\frac{\partial^2 B_1}{\partial y^2} + \frac{(4\beta+1)}{4\beta}k(|B|^2 - |B_0|^2)B_0 + \frac{(4\beta+1)}{4\beta}k|B|^2 B_1 = 0. \tag{3}$$

Here B is the sum of the fields due to main Alfvén wave and the perturbation ($B = B_0 + B_1$). In order to obtain the solution of (3), we express the perturbation field as

$$B_1 = B_{10}(y, \xi)\exp(-ikS_1(y, \xi)). \tag{4}$$

Here B_{10} and the eikonal (S_1) are real functions of y and ξ.

Using (4) in (3), we obtain the following equations, after separating the real and imaginary parts:

$$\frac{\partial S_1}{\partial \xi} + \frac{1}{2(\beta-1)}\left(\frac{\partial S_1}{\partial y}\right)^2 + \frac{(4\beta+1)}{4\beta}k(2B_{00}^2\cos^2(\phi) + |B|^2) + \frac{1}{2k^2(1-\beta)}B_{10}\frac{\partial^2 B_{10}}{\partial y^2} = 0. \tag{5}$$

and

$$\frac{\partial B_{10}}{\partial \xi} - \frac{1}{(1-\beta)}\frac{\partial B_{10}}{\partial y}\frac{\partial S_1}{\partial y} - \frac{B_{10}}{2(1-\beta)}\frac{\partial^2 S_1}{\partial y^2} + \frac{(4\beta+1)}{4\beta}kB_{00}^2 B_{10}\sin(2\phi) = 0. \tag{6}$$

Here B_{00} is amplitude of the main Alfvén wave and φ is the angle between the main Alfvén wave field and the perturbation field. The value of φ depends on the phase angle between the main Alfvén wave field and that of the perturbation field at $\xi = 0$, and the phase shift introduced in the perturbation field due to the nonlinearity in the medium. Using the paraxial approximation ($y \ll r_0 f_1$), one can write the solution

https://doi.org/10.1017/S0022377805003843 Published online by Cambridge University Press

of (5) and (6) as (Akhmanov et al. 1968)

$$B_{10}^2 = \frac{B_{100}^2}{f_1} \exp\left(-\frac{y^2}{r_0^2 f_1^2}\right) \exp(-2k_i\xi). \tag{7}$$

Here the growth rate is given by

$$k_i = \frac{(4\beta+1)}{4\beta} k B_{00}^2 \sin(2\phi),$$

and

$$S_1 = \beta_1(\xi)\frac{y^2}{2} + \phi_1(\xi), \tag{8}$$

where

$$\beta_1(\xi) = (\beta-1)\frac{1}{f_1}\left(\frac{df_1}{d\xi}\right). \tag{9}$$

Here f_1 is the dimensionless beam-width parameter of the perturbation field, which depends on ξ. The inverse of β represents the radius of the curvature of a wavefront. Using (7) and (8), we obtain the following equation for f_1, after equating the coefficients of y^2 in (5):

$$\frac{d^2 f_1}{d\xi^2} = \frac{1}{k^2(1-\beta)^2 r_0^4 f_1^3} - \frac{[(4\beta+1)]}{2\beta(1-\beta) r_0^2 f_1^{3/2}} B_{00}\cos(\phi) B_{100}\exp(-k_i\xi). \tag{10}$$

In the right-hand side of (10), the first term accounts for the diffraction of the perturbation because of its finite transverse size, while the second term accounts for the nonlinearity. The nonlinear term is governed by the fields of the main Alfvén wave and that of the perturbation, the phase angle between these two fields, the plasma beta and the spatial growth rate k_i. A self-trapping mode is obtained when the two terms in the right-hand side of (10) balance each other. The wave then propagates without convergence or divergence (namely $f_1 = 1$). The expressions for the critical magnetic field ($B_{100(\mathrm{cr})}$) or the critical value of transverse size [$r_{0(\mathrm{crit})}$] of perturbation is obtained by balancing the two terms in the right-hand side of (10). The expression for the critical magnetic field of the perturbation obtained from (10) is

$$B_{100(\mathrm{cr})} = \frac{2\beta}{[(1-\beta)(4\beta+1)]} \frac{1}{B_{00}\cos(\phi)} \frac{1}{k^2 r_0^2} \tag{11}$$

and the critical value of the transverse size of the perturbation is obtained from (10) as

$$r_{0(\mathrm{cr})} = \left(\frac{2\beta}{[(1-\beta)(4\beta+1)]k^2 B_{00} B_{100}\cos(\phi)}\right)^{1/2}. \tag{12}$$

Now we would like to make an estimate of this critical magnetic field in two astrophysical situations.

(1) Solar wind: typical Solar wind parameters are $T = 1.5\times10^5$ K, $B_0 = 7.2\times10^{-5}$ G, proton (and electron) density = 5 particles cm^{-3} and $\beta = 0.5$. We find that $v_A = 7.0\times10^6$ cm s^{-1} and $\Omega_I = 0.7$ rad s^{-1}.
For these parameters, the characteristic normalizing distance comes out to be $L \approx 40\times10^6$ cm, the characteristic normalizing wavenumber $\approx 2.5\times10^{-8}$ cm^{-1} and the characteristic normalizing frequency ≈ 1.1 s^{-1}.

https://doi.org/10.1017/S0022377805003843 Published online by Cambridge University Press

(2) Solar corona: for the Solar corona, typical parameters are $T = 0.4 \times 10^6$ K, $B_0 = 32$ G, proton (and electron) density $= 10^8$ particles cm^{-3}, $\beta = 1.35 \times 10^{-4}$. From these we find that $v_A = 6.98 \times 10^8$ cm s^{-1} and $\Omega_I = 3.065 \times 10^{-5}$ rad s^{-1}.

For these parameters, the characteristic normalizing distance comes out to be $L \approx 9.114 \times 10^3$ cm, the characteristic normalizing wavenumber $\approx 1.097 \times 10^{-4}$ cm^{-1} and the characteristic normalizing frequency $\approx 1.305 \times 10^{-5}$ s^{-1}.

3. Discussion

In this paper we have studied the nonlinear coupling between the perturbation and the plane Alfvén wave. The perturbation takes energy from the main Alfvén wave, may grow and finally can result in filament (hot spot) formation. For the filamentation, the critical magnetic field is very important and the value of magnetic field of fluctuations should be more than the critical value. Using (11), we have calculated the critical magnetic field for typical parameters of the Solar wind and the Solar corona.

Figure 1(a) depicts the variation of the critical magnetic field of the perturbation against its transverse size (r_0) for different values of β in the case of the Solar wind. It is evident from the figure that for a particular value of β, as the transverse size increases, the value of the critical field decreases. This can be explained using (10). As the transverse size (r_0) increases, the nonlinear term (the second term in the right-hand side of (10)) dominates over the diffraction term (the first term in the right-hand side of (10)). Hence, from (10), the critical field required to balance the nonlinear and diffraction terms decreases. We can also see from Fig. 1(a) that as the value of β increases, the critical field increases. In (10), for higher values of β, the nonlinear term decreases and hence the critical field increases.

A similar trend for the critical magnetic field, as in Fig. 1(a), is obtained for typical parameters of the Solar corona, as shown in Fig. 1(b). Figure 1(b) displays the variation of the critical magnetic field of the perturbation against its transverse size for different values of β, for the Solar corona parameters. As we can see from the figure, the magnitude of the critical magnetic field for the Solar corona parameters is much lower than for the Solar wind parameters. For the Solar corona, the value of the background field is much more than the Solar wind. This decreases the value of β ($\beta = 8\pi n_0 T / B_0^2$), hence decreases the value of the critical field.

Figure 2(a) exhibits the critical magnetic field of the perturbation against its transverse size for different values of the main Alfvén wave field for the Solar wind parameters. From this figure, we see that as the main Alfvén wave field increases, the critical field decreases. With the increase in the main Alfvén wave field, the nonlinear term increases, hence results in a decrease in the critical field. Figure 2(b) shows the critical field against the transverse size for different values of the main Alfvén wave field and for the Solar corona parameters.

Figures 3(a)–(c) illustrate the intensity pattern of the perturbations at different distances along the direction of propagation, but in a direction (plane) transverse to the direction of propagation, for the Solar wind for different values of β. Figure 3(b) is the case for $\beta = 0.5$. As observed in this figure, filamentary structures are seen at different locations in space. This can be explained using (10). When the magnetic field of the perturbation is more than its critical magnetic field, the nonlinear term dominates and the value of f_1 decreases with the distance of the propagation.

https://doi.org/10.1017/S0022377805003843 Published online by Cambridge University Press

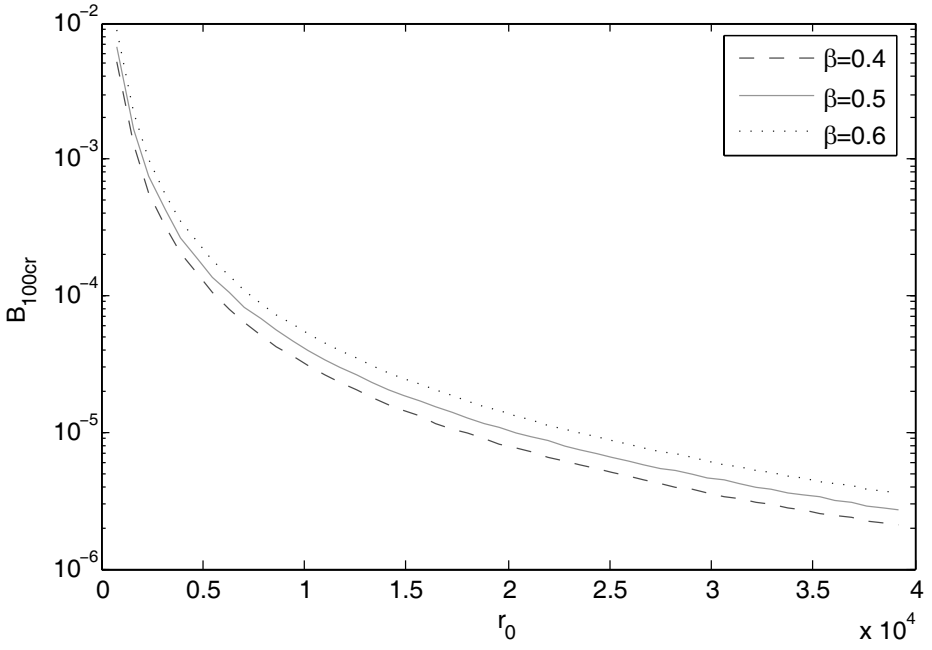

(a)

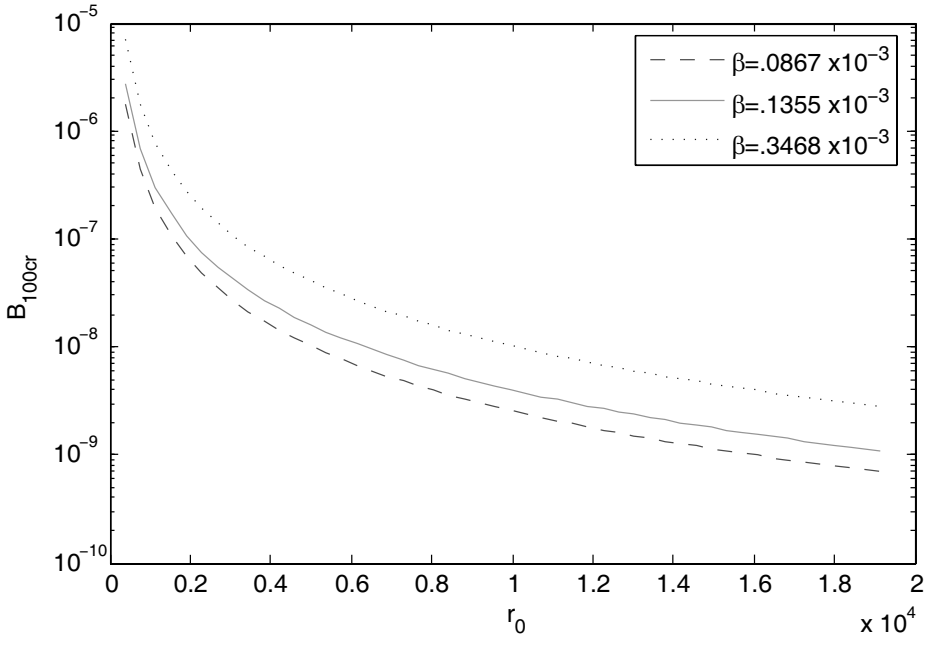

(b)

Figure 1. (a) The variation of the critical magnetic field (normalized against background field) of the fluctuation against its transverse size (r_0) for different values of β in the case of the Solar wind. (b) The variation of the critical magnetic field (normalized against background field) of the fluctuation against its transverse size (r_0) for different values of β in the case of Solar corona.

https://doi.org/10.1017/S0022377805003843 Published online by Cambridge University Press

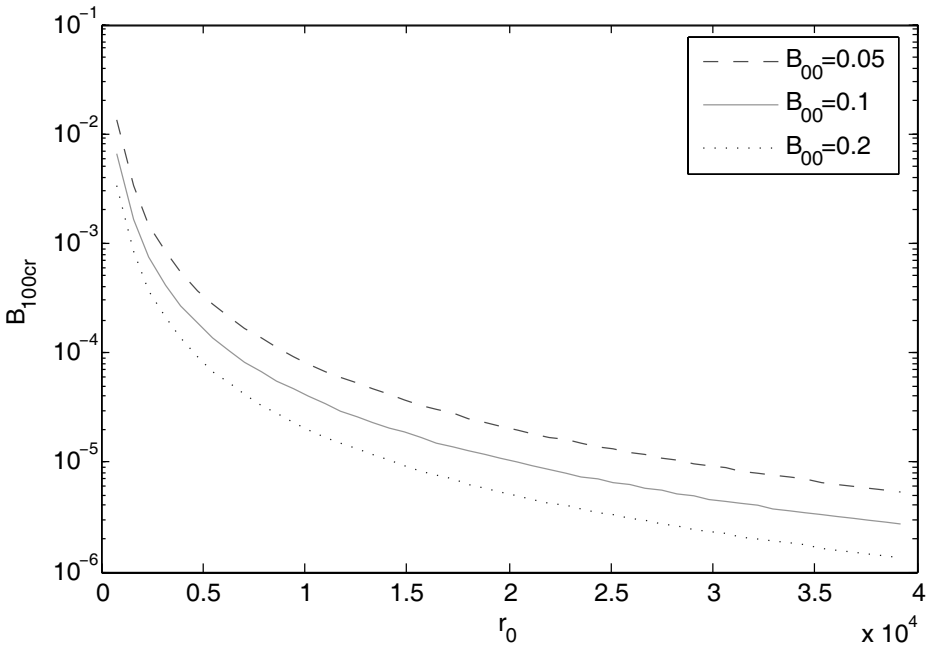

(a)

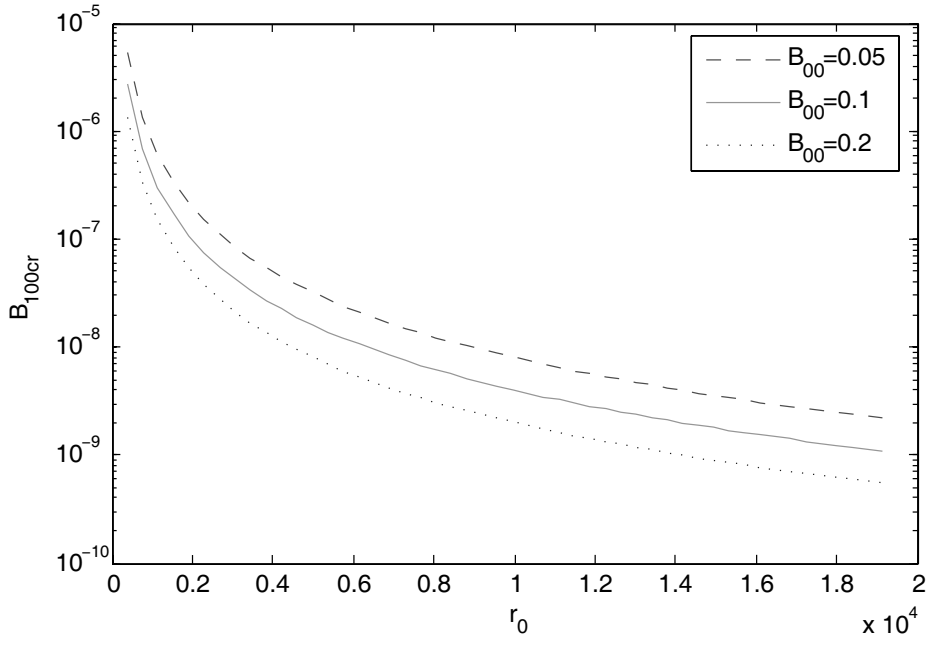

(b)

Figure 2. (a) The variation of the critical magnetic field (normalized against background field) of the fluctuation against its transverse size (r_0) for different values of main Alfvén wave field B_{00} in the case of the Solar wind. (b) The variation of the critical magnetic field (normalized against background field) of the fluctuation against its transverse size (r_0) for different values of main Alfvén wave field B_{00} in the case of the Solar corona.

https://doi.org/10.1017/S0022377805003843 Published online by Cambridge University Press

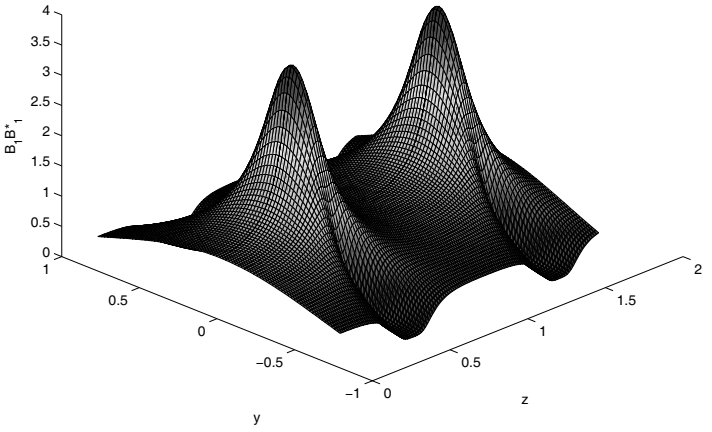

(a)

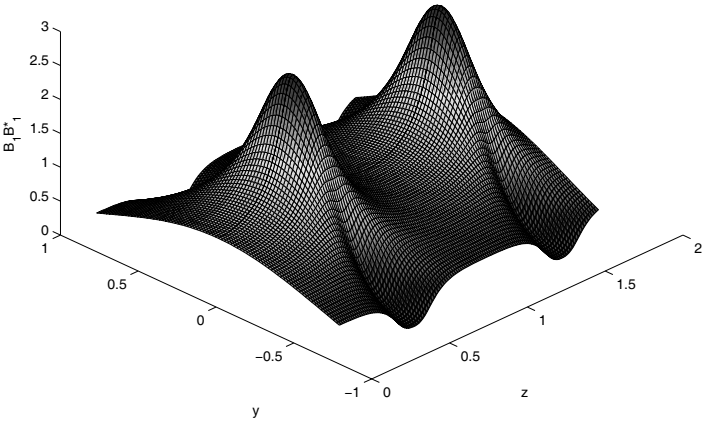

(b)

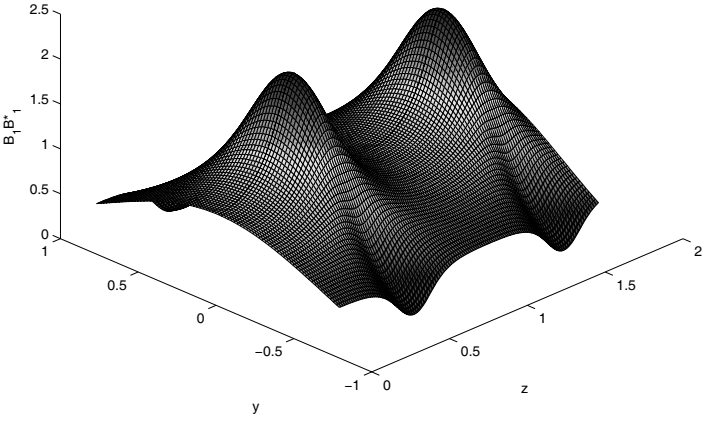

(c)

Figure 3. The intensity distribution of perturbations (normalized against background field) at different distances along the normalized direction of propagation z ($\equiv \xi/R_{\rm d}$, $R_{\rm d} = kr_0^2$) for fixed $B_{00} = 0.1$ in the case of the Solar wind and for fixed: (a) $\beta = 0.4$; (b) $\beta = 0.5$; and $\beta = 0.6$.

https://doi.org/10.1017/S0022377805003843 Published online by Cambridge University Press

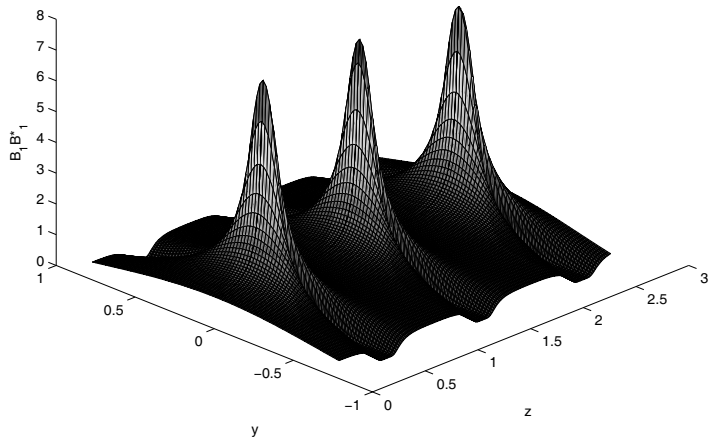

(a)

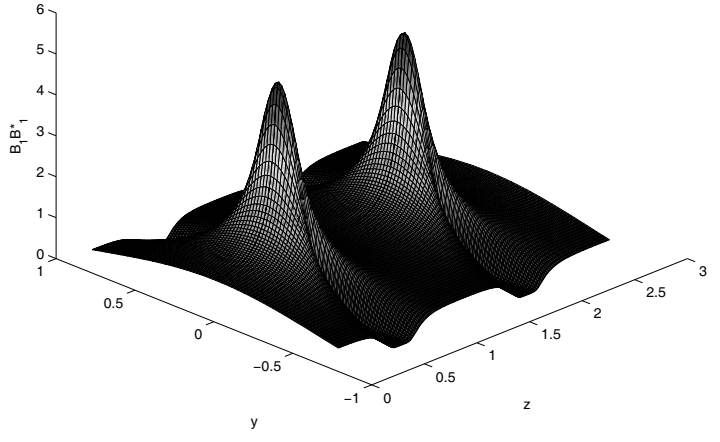

(b)

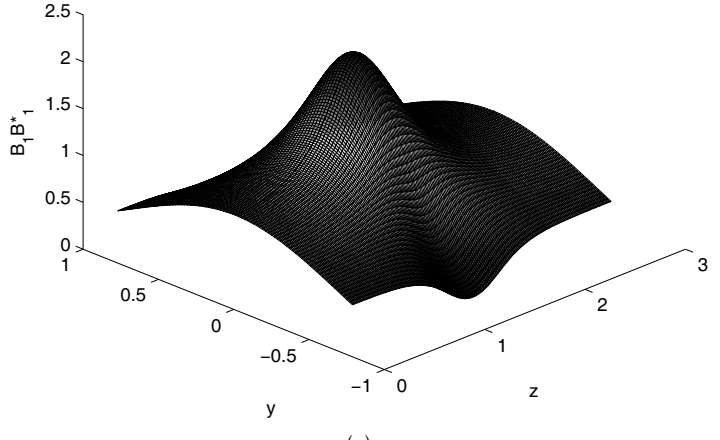

(c)

Figure 4. The intensity distribution of perturbations (normalized against background field) at different distances along the normalized direction of propagation z ($\equiv \xi/R_{\rm d}$, $R_{\rm d} = kr_0^2$) for fixed $B_{00} = 0.1$ in case of the Solar corona and for fixed: (a) $\beta = 0.0867 \times 10^{-3}$; (b) $\beta = 1.355 \times 10^{-3}$; and (c) $\beta = 0.3468 \times 10^{-3}$.

https://doi.org/10.1017/S0022377805003843 Published online by Cambridge University Press

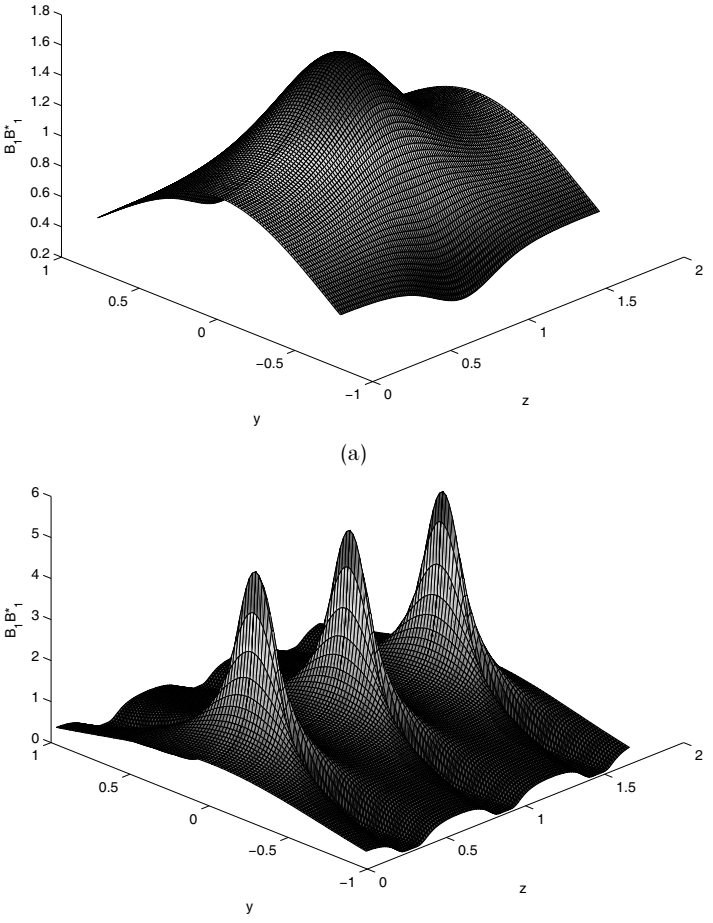

Figure 5. The intensity distribution of perturbations (normalized against background field) at different distances along the normalized direction of propagation z ($\equiv \xi/R_{\rm d}$, $R_{\rm d} = kr_0^2$) for fixed $\beta = 0.5$ in the case of the Solar wind and for fixed: (a) $B_{00} = 0.05$; and (b) $B_{00} = 0.2$.

However when f_1 becomes very small, the diffraction term starts dominating and f_1 starts diverging. Therefore, f_1 increases with the distance of the propagation until f_1 becomes so large that the diffraction term becomes smaller in comparison with the nonlinear term. Then, f_1 again decreases due to the nonlinear effects, until it becomes so small that the diffraction term again dominates and f_1 starts diverging and this process repeats. Hence, the perturbation attains a certain minimum beam-width parameter (f_1), and the intensity of the perturbation in these small size structures becomes very high.

Figures 3(a)–(c) display the intensity distribution of the perturbation for β values 0.4, 0.5 and 0.6, respectively, in the case of the Solar wind. As observed in these figures, intensity of the filaments increases with decreasing values of β. This can be explained as follows. With decreasing β, the nonlinear term increases; hence the nature of f_1 is more affected through the nonlinear term in (10). An increase in the nonlinear term causes more rapid changes in f_1 with ξ. Also, the balancing of the

https://doi.org/10.1017/S0022377805003843 Published online by Cambridge University Press

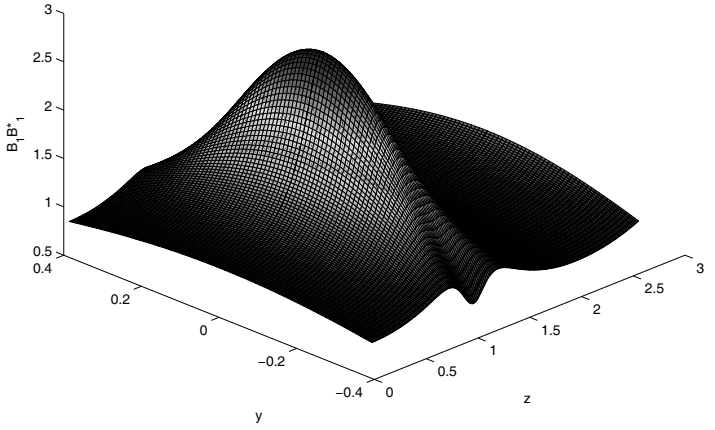

(a)

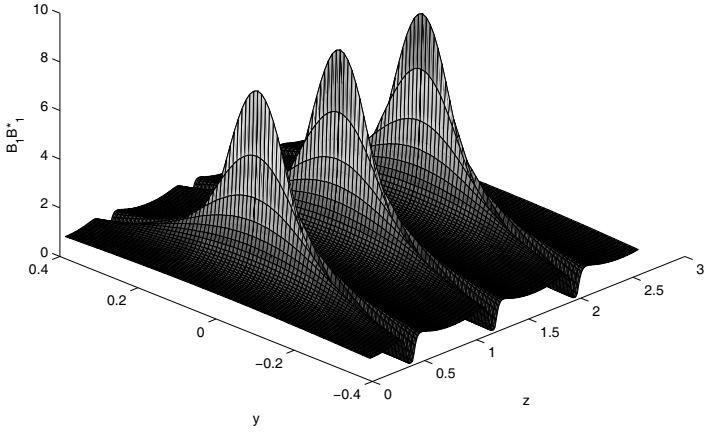

(b)

Figure 6. The intensity distribution of perturbations (normalized against background field) at different distances along the normalized direction of propagation z ($\equiv \xi/R_{\rm d}$, $R_{\rm d} = kr_0^2$) (for fixed $\beta = 1.355 \times 10^{-3}$) in the case of the Solar corona and for fixed: (a) $B_{00} = 0.05$; and (b) $B_{00} = 0.2$.

nonlinear and diffraction terms takes place at lower f_1. This results in the formation of more intense filaments with earlier formation and less separation between them. The same behavior (as in Figs 3(a)–(c)) is observed for different values of β in the Solar corona, as shown in Figs 4(a)–(c).

Finally, we have studied the effect of the main Alfvén wave field (B_{00}) on the intensity distribution of perturbations. Figures 3(b), 5(a) and (b) show the intensity distribution of perturbation for the main Alfvén wave field (B_{00}) for values 0.1, 0.05 and 0.2, respectively, for the Solar wind. As seen in the figures, with increasing B_{00}, the number of filaments as well as their intensity increases. This is because of the increase in the nonlinear term in (10). The same is observed with changes in B_{00} for the Solar corona as shown in Figs 4(b), 6(a) and (b).

The above results show that the perturbations present on the main Alfvén wave may lead to the filamentation process. These filaments may further act as a source of decay waves, as well as a source of further collapse of the main Alfvén wave,

https://doi.org/10.1017/S0022377805003843 Published online by Cambridge University Press

changing the spectrum of the Alfvénic turbulence. Hence, the spectral index (slope) is also expected to change. This mechanism may be useful in the coronal heating, may even have some relevance about the initiation of turbulence in the Solar wind and, specifically at the small scales, may provide the nonlinear means of dissipation and heating of the ambient Solar wind plasma. Although rough estimates to find the enhancement in the ion temperature have been made earlier, rigorous models based on a quasi-linear theory should be used to find these estimates. This will require the wavenumber spectrum of the excited Alfvén waves in hot filaments, calculating the velocity space diffusion coefficient and using this in the Fokker–Planck equation (Marsch 1998). Perhaps the discrepancies between the experimentally measured spectra and theory can be explained by using these phenomena.

Acknowledgement

M. Malik is grateful to CSIR for granting the fellowship for the present research work. This work is partially supported by DST (India).

References

Akhmanov, S. A., Sukhorukov, A. P. and Khokhlov, R. V. 1968 Self focusing and diffraction of light in a nonlinear medium. *Sov. Phys. Usp.* **10**, 609.

Champeaux, S., Passot, T. and Sulem, P. L. 1997 Alfvén wave filamentation. *J. Plasma Phys.* **58**, 665.

Champeaux, S. et al. 1998. Transverse collapse of Alfven wavetrains with small dispersion. *Phys. Plasmas* **5**, 100.

Champeaux, S., Passot, T. and Sulem, P. L. 1999 Dissipation of weakly dispersive Alfvén wave. *Phys. Plasma* **6**, 413.

Del Zanna, L., Velli, M. and Londrillo, P. 2001 Parametric decay of circularly polarized Alfvén waves: multidimensional simulations in periodic and open domains. *Astron. Astrophys.* **367**, 705.

Ferraro, V. C. A. 1955 Hydromagnetic waves in a rare ionized gas and galactic magnetic fields. *Proc. R. Soc. (London)* A **233**, 310.

Goldstein, M. L., Roberts, D. A. and Matthaeus, W. H. 1995 Magnetohydrodynamics turbulence in the solar wind. *Annu. Rev. Astron. AstroPhys.* **33**, 283.

Kruer, W. L. 1988 *The Physics of Laser Plasma Interactions*. Red wood City CA: Addison-Wesley.

Lavender, D., Passot, T. and Sulem, P. L. 2001 Transverse collapse of low frequency Alfvén waves. *Physica* D **152–153**, 694.

Lavender, D., Passot, T. and Sulem, P. L. 2002 Transverse dynamics of dispersive Alfvén waves. I. Direct numerical evidence of filamentation. *Phys. Plasmas* **9**, 293.

Marsch, E. 1998 Cyclotron heating of the Solar corona. *Astrophys. Space Sci.* **264**, 63.

Spangler, S. R. 1990 Kinetic effects on Alfvén wave nonlinearity. II. The modified nonlinear wave equation. *Phys. Fluids* B **2**, 407.

Spangler, S., Fuselier, S., Fey, A. and Anderson, G. 1988 An observational study of MHD wave-induced density fluctuations upstream of the Earth's bow shock. *J. Geophys. Res.* A **93**, 845.

Tu, C.-Y. and Marsch, E. 1995 *MHD Structure Waves and Turbulence in the Solar Wind: Observation and Theories*. Dordrecht: Kluwer.